Concepts of Catalysis

M.K. Carter

Carter Technologies, Lincoln, CA 95648

A unitary transformation of the catalyst wave function, $Uc=c$, shows the essential backbone to be linear and the highest filled molecular energy levels to be degenerate. Catalysis is redefined: **catalysis is a barrier free transformation of one electronic configuration to another**, changing reactants to products. A six-step catalyst design method is presented.

Abstract

The field of catalysis is well known from an experimental perspective, but its fundamental underpinnings are missing. Fundamentals of catalysis are developed from a quantum perspective for a reactant and an embryonic product requiring a catalyst backbone to be at least two-fold degenerate. The article addresses the symmetry of wave functions and simple energy computations for selected catalyst complexes. Catalysis is redefined: a barrier free transformation of one electronic configuration to another, changing reactants to products. A six-step method has been established sufficient for design of catalysts at the molecular level with examples of Fischer-Tropsch catalysis [Co(HCN)$_2$•Fe(HCN)$_2$•Co(HCN)$_2$] and air oxidative destruction [Fe(CN)$_2$L•Fe(CN)$_2$L] of aliphatic hydrocarbons both at ambient temperature.

I. Introduction

Catalysts and enzymes are reported[1] to aid reactions by binding to reactants and lowering the energies of transition states. Molecular models effecting a lowered transition state energy of enzymatic catalysis reside at the center of a controversy as some say[1] the mechanism is electrostatic bonding, quantum mechanical tunneling, coupled molecular motions, low-barrier hydrogen bonds or near attack conformations. If catalysis is a quantum effect, then a more fundamental description of its principles is needed. Consider the function of a catalyst. Linus Pauling taught[2] that a catalyst exhibits the property of accelerating a chemical reaction without undergoing significant change itself. He stated, "It is thought that catalysts speed up reactions by bringing the molecules reacting together and holding them in configurations favorable to reaction." Cotton and Wilkinson[3] considered the process rather than the species. They stated that homogeneous catalytic reactions in solution are commonly very complex and proceed by way of linked chemical reactions in a closed cycle involving different metal species. These ideas offer a picture of what is achieved but not the mechanism.

The goal of this work is to present a quantum basis for catalysis and to establish the electronic concepts of catalysis sufficient for design of active catalysts at the molecular level. The following sections address electronic configuration of a catalyst, required molecular symmetry, relative energies of selected catalyst-reactant complexes, a trial transition probability, stabilization of a catalyst against oxidation and two examples of catalyst design.

Chemical reactions occur provided the thermodynamic free energy is negative[4], that is, product energy lies lower than reactant energy. Allowed reactions that do not readily proceed through a transition state to products are said to be subject to a kinetic barrier[5], however in this work a catalyst may be viewed as opening a symmetry based transition gate allowing the reactant to penetrate through the kinetic barrier[6].

A catalyst is held to be a specific substance that facilitates a chemical reaction or isomerization of associated reactants. Catalytic activity is centered on a single atom or group of transition metal atoms such that the reactant becomes associated with this site and an embryonic product simultaneously forms there from. An embryonic product is defined as a reactant whose atoms remain located at their initial coordinates but whose electronic configuration has changed such that bonding electrons temporarily occupy orbitals of the transition metal. It will be shown that a reactant and the embryonic product simultaneously represent two different bonding configurations. This implies that degeneracy exists such that both configurations have the same energy. A true catalyst provides an orbital pathway for a reactant to proceed to an embryonic product. Once this electron shift has occurred the atoms of the embryonic product reposition (vibrate) to comply with the newly established

electronic configuration such that the thermodynamic change in free energy for the reaction is negative; i.e., reactants automatically proceed to products in the presence of a catalyst. In other words, a reactant becomes associated with a catalytic site where a chemical transformation is facilitated. Since the change in free energy is negative then a reactant may be considered to be in a chemically excited state relative to the product where the product lies at lower energy than the embryonic product. Thus, the act of catalysis may be treated as a radiationless[7] stimulated emission – a natural transition from one electronic configuration to another.

Consider a molecular model consisting of a transition metal catalyst and an associated reactant such that the catalyst is represented by its ground state eigenfunction, ψ_c, having energy E_c, and the reactant by its ground state eigenfunction, ψ_r, having energy E_r. Further, let the geometric positions of the atoms of the reactant represent a basis for both the reactant and its embryonic product where only a shift in electronic bonding distinguishes one from the other. Here the wave function ψ_{ep} represents the ground state of the embryonic product having energy E_{ep} such that $E_{ep} = E_r$ constituting a degenerate electronic state. The Born-Oppenheimer approximation[8] allows the electronic wave function to be cast with specific inter-nuclear distances, assuming all nuclei to remain in fixed positions since electronic motion is orders of magnitude faster than nuclear motion. Thus, degenerate eigenfunctions of a reactant and its simultaneous embryonic product constitute a natural path for catalyzed reactants to proceed to products.

It is of interest to address the anticipated energy of association of an organic reactant with a catalyst. Consider the known chemical bond energies of C-C, C-H and hydrogen bonds for organic compounds. Extrema bond energies of -60 kcal/mol (-251 kJ/mol) for phenyl-t-butyl nitrile and -116 kcal/mol

(-485 kJ/mol) for hexafluoroethane establish a range for C-C bonds, and extrema energies of -76 kcal/mol (-318 kJ/mol) for trimethylpropane and -105 kcal/mol (-438 kJ/mol) for methane establish a range for

C-H bonds[9]. Thus, a span of -60 to -116 kcal/mol (-251 to -485 kJ/mol) represents the range for the majority of organic C-H and C-C bonds. Weaker hydrogen bonds typically lie in a range of 0 to

-5 kcal/mol (0 to -21 kJ/mol). The association energies between a catalyst and its reactant are anticipated to lie in the intermediate -5 to -60 kcal/mol (-21 to -251 kJ/mol) range so that formation a catalyst-reactant complex may be energetically favored while formation of an organic product remains more highly favored. The following sections address the symmetry of wave functions, simple energy computations for selected catalyst complexes, introduction of a six-step method for designing catalysts at the molecular level and examples of catalysts designed using these methods.

II. Catalyst Configuration

Let r represent the column vector wave function of a reactant and let p represent the column vector for a product. There is a fundamental postulate stating that to every observable there corresponds an operator[10]. Transformation of the function r to a related function p is expressed by a unitary matrix operation as $Ur = p$ so both the symmetry of the wave functions and the length of the vectors are preserved. By definition, a unitary operator is self-adjoint so $U^\dagger = U^{-1}$ and $U^\dagger U = UU^\dagger = E$ for which E is a unit diagonal matrix. Let

U_j represent the elements of a single column of the unitary operator U. The Hermitian scalar product of two such columns[11] as $U_j^\dagger U_k$ in $\Sigma_l U_{lj}^* U_{kl} = \Sigma \delta_{jk}$ and a similar relationship holds for pairs of rows, demonstrating the vectors are orthogonal and normalized. Hence the rows and columns of a unitary matrix of order n form a set of n mutually orthogonal unit vectors in Hermitian space. Since $Ur = p$ and $r^\dagger U^\dagger = p^\dagger$ it may be seen that a transformation by a unitary matrix leaves a quadratic form invariant as $r^\dagger U^\dagger Ur = r^\dagger r$

$= p^\dagger p$. The eigenvalues of a unitary matrix may be real or complex but of absolute value 1. Let λ_i be an eigenvalue of U then, $Ur = \Pi_i \lambda_i r$, and $(Ur)^\dagger Ur = r^\dagger r = \Pi_{ik} \lambda_i^* \lambda_k r^\dagger r$. Since $r^\dagger r$ is real and does not vanish[12], then $\Pi_{ik} \lambda_i^* \lambda_k = 1$.

The expression $Ur = p$ indicates a relation between r and p but does not reveal its symmetry characteristics. Catalysis may be viewed as a transformation converting a reactant to its embryonic product where the catalyst assists in the transformation such that the catalyst ends in its original state. It is useful to re-express $Ur = p$ as $U = pr^{-1} = pr^\dagger$ where $r^\dagger$ is a transposed column vector, a row vector, for a real function. A catalytic transformation may be expressed as $Ucr^\dagger = cp^\dagger$ where the vector c represents the catalyst wave function and $cp^\dagger$ results in a matrix. The resultant quadratic form becomes $r^\dagger c^\dagger U^\dagger Ucr = r^\dagger c^\dagger cr = p^\dagger c^\dagger cp$. Catalysis may be represented as $Uc = d$ but the resultant d is identical to the representation of the original catalyst c resulting in the equation

$$Uc = c$$

Thus, other than the identity operation for which U = 1, then U must be a symmetry transformation operation such that c remains unaltered. Further, the symmetry group is required to possess at least one axis of

symmetry, meaning the catalytic backbone is linear and its highest bonding orbital is inherently degenerate to accommodate simultaneous eigenfunctions of a reactant and its embryonic product.

The symmetry requirement indicates the molecular axis of the electronically significant structure of the catalyst will be linear. For example, a set of atoms bonded where M is a transition metal and Y is any appropriate electronegative atom is expressed by Y-M-Y, such as Co-Fe-Co, which is described as being in a linear geometric configuration. Should the molecule Y-M-Y be inherently non-linear, such as manganese chloride, Cl-Mn-Cl, it may still exhibit catalytic activity during that fraction of time its bending vibration carries it through a linear geometric configuration. This concept may be represented in general terms as follows. Theorem 1: a catalyst contains a symmetry axis aligned with a linear string of atoms where the active site is a transition metal. Tolman et al[13] have reported a di-copper di-oxygen complex that reversibly breaks oxygen bonds, a catalytic example of Theorem 1. A related di-iron enzyme oxidation model compound was reported by Que and Lipscomb et al[14]. The catalytic center of nitrous oxide reductase, which displays a novel butterfly shaped cluster of four copper ions (two strings of two copper ions), reportedly represents an example of a metal-metal bond in nature[15]. Methane mono-oxygenase enzyme, which air oxidizes methane at ambient temperature, reportedly contains two adjacent iron complexes each with an Fe-Fe bond distance of 340 pm[16,17] as probable catalytic sites. A palladium dimer bound by means of a halide bridge has been reported to facilitate a fast reaction of aryl halides[18]. Catalytic effects of atomic alignment in complex arrays of crystals has been expressed by MO calculations, conducted for dissociation of CO on a 100 face of Fe_{12} crystals[19,20], and by other works addressing linear atomic arrays in single crystal surfaces as found in heterogeneous catalysts. Poly-centered metal carbonyl clusters have been shown to initiate Fischer-Tropsch catalytic hydrogenation of carbon monoxide in formation of C_3-C_{30} alkanes[21] while the monomeric species were inactive[22-24]. An interesting, alternative approach to active heterogeneous catalysis was achieved by imbedding one metal in a field of a different metal through formation of a Co-Mn alloy[24-26]. Several reports of improved performance of Fischer-Tropsch catalysis are based upon modification of an iron catalyst with approximately 5 to 10 percent copper[27,28]. These modified catalysts may also conform to the proposed theorem and related representations possibly in the form of

Cu-Fe or Cu-Fe-Cu as listed in Table 4 for linear catalysts. Refer to tables 5 and 6 for second and third row transition metal catalyst backbone structures. A number of workers have investigated Fischer-Tropsch catalytic conversion of synthesis gas to higher hydrocarbons on finely divided iron catalysts containing other metals. Analysis of the catalyst residues indicated iron carbide, Fe_5C_2, was present that was proposed[29] to be a possible active species. Recently enhanced catalysis was observed on a bimetallic
Pd-Au interface[30] using super-resolution imaging during catalytic disproportionation.

Linear metallic strings are not the only species to fulfill the symmetry requirements. Single metal catalysts with attached ligands, represented by L-M-L' for which L and L' indicate similar bonded ligands or anions, are some of the simplest molecules to conform to theorem 1. For example, $RhCl(PPh_3)_3$, the Wilkinson reduction catalyst, the $Ru(CO)_3(PPh_3)_2$ hydroformulation catalyst[31] and the $Co(OAc)_2$ toluene to benzoic acid oxidation catalyst[32] also fulfill the symmetry requirements during the linear portion of their vibrational motion.

III. Molecular Symmetry Requirements

Enzymes have been described[1] as lowering the energy of a transition state, a classical concept. Kinetic activation energy of a transition state may be represented by a distribution[33] of bonding energies resulting in an average barrier height (energy) greater than zero centered on the reaction coordinate. In quantum considerations, symmetry operations select the critical contribution to the transition state specifying the optimum wave function(s) and populating those states of highest transition probability, therefore, of minimum energy. Thus, symmetry allows the catalyst reactant complex to simultaneously achieve electron bonding as its degenerate embryonic product provides a path for conversion of a reactant to an allowed product. Without these energy-free symmetry gateways the rate of catalysis could be severely restricted by thermal and kinetic barriers.

Symmetry of a catalyst addresses chemical bonding of the transition metals (typically a pair or trio) and those atoms directly bonded thereto. Catalyst molecules become immersed in a sea of surging reactant and possibly solvent molecules. Once a reactant molecule becomes coordinated with a catalytic transition metal atom, then the reactant transitions to an embryonic product to initiate product formation.

It is apparent that the backbone of a catalyst is linear and the wave functions of a reactant and its embryonic product belong to a degenerate state. The symmetry group that best describes the molecular model places restrictions on the wave functions sufficient to determine their form. The Schrödinger equation, and hence the Hamiltonian operator H in the equation $H\psi=E\psi$, are invariant under group symmetry operations; thus, if R_i represents the ith symmetry operation of a group then $R_1R_2R_3 ... R_i H R_1R_2R_3 ... R_i \psi = E R_1R_2R_3 ... R_i \psi$ which becomes $H R_1R_2R_3 ... R_i \psi = E R_1R_2R_3 ... R_i \psi$ or more simply $H^\#\psi = E^\#\psi$ for which $^\#\psi$ is the specific symmetry constrained wave function that describes the reactant-catalyst association. The operators R_i

commute[34] allowing for expansion of the wave function as a series of simultaneous eigenfunctions[35] of the symmetry operators. Thus, if $^{\#}\psi$ represents a reactant + catalyst then it, or some linear portion there of, also represents a degenerate embryonic product + catalyst. In general, a symmetry constrained degenerate wave function may be expressed as a linear combination of independent functions as $R_1\psi_i = \Sigma_k D(R)_{ki}\psi_k$ for which $D(R)$ is the transformation matrix associated with symmetry operator R. When the complete set of irreducible representations is obtained each one corresponds to an eigenvalue for a specific molecular symmetry.

A model of a tri-atomic linear catalyst $M_e - M_i(m\text{-}n)_4 - M_e$ with four *m-n* polar reactants symmetrically positioned around the central metal atom M_i, having axes co-parallel with the metal string axis, forms a full six coordinate compliment bond set. Here *e* represents the external atoms and *i* represents the internal atom of the complex. Since the axes of *m-n* are parallel to the linear axis of $M_e - M_i - M_e$, then this molecular configuration belongs to the C_{4v} symmetry group, refer to figure 1, and the molecular wave function may be described by the two-dimensional irreducible representation *E*. Identification of the symmetry of a specific reactant-catalyst association accurately determines the wave functions that describe the molecular interaction. Other acceptable symmetries also exist as considered later in this section.

Reactant(s) associated with a catalyst may be classed as either polar or non-polar. Polar carbon monoxide molecules associated with an $M_e - M_i - M_e$ catalytic backbone may be bonded as shown in figure 1, corresponding to the C_{4v} symmetry group (unlike wagon wheel shaped iron penta-carbonyl of figure 3).

Semi-empirical computations[36] demonstrated the tetracarbonyl complexes of manganese, iron and cobalt, with carbon monoxide molecules oriented as shown in figure 1, produced bonding while complexed carbon monoxide in alternate anti-parallel orientation, as shown in figure 2, did not produce significant bonding for manganese or cobalt.
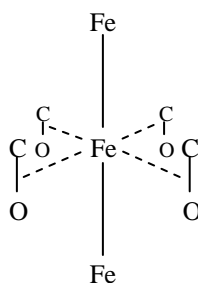
Figure 1. A Representation of Fe-Fe(*C-O*)$_4$-Fe In C_{4v} Symmetry.

The four C-O molecules associated with the catalyst M_e-M_i(*C-O*)$_4$-M_e, shown in figure 1, form a group described by the *E, 2C$_4$, C$_2$, 2σ_v* and *2σ_d* classes of symmetry operations. The direct product of irreducible representations describing the polarizability matrix, α, is $\Gamma(A_1)$ x $\Gamma(E) = \Gamma(E)$ which is also irreducible. The E irreducible basis is the only two-dimensional representation that accommodates the degeneracy of states required to describe catalysis. Thus, there must exist two electronic configurations, one that represents bonding configuration A while the other describes bonding configuration B. The transformation from a reactant belonging to one degenerate level (E_A) to an embryonic product belonging to the other (E_B) may be described as an electron shift. The theorem[37] governing elements of the matrices that constitute the irreducible representations of a group may be stated as

$$\Sigma_R \Gamma_i(R)_{mn}{}^* \Gamma_j(R)_{m'n'} = (h/\sqrt{l_i l_j})\ \delta_{ij}\ \delta_{mm'}\ \delta_{nn'}.$$

where the sum of the squares of the characters equals the order of the group, that is

$$\Sigma_i \Gamma_i(R)_{mn}{}^2 = h$$

The C_{4v} symmetry group character table is reproduced in table 2 for convenience. It is observed that the C_{4v} character table is a sub-set of the D_{4h} character table with similar characteristics. A representation for the set of four carbon monoxide ligands is given as Γ_{CO} and a representation for the Fe$_3$ backbone or linear string is given as Γ_{Fe}. Since there are two kinds of molecules in the symmetry group the preferred basis of each molecule may be determined from the individual groups directly. Carbon monoxide belongs to the $C_{\infty v}$ symmetry group and its bonds are identified as π-2sp(z), σ-2p(x) and σ-2p(y). The catalyst molecule, M_e-M_i-M_e, belongs to the

$D_{\infty h}$ symmetry group (as do M-M, M-M-M-M and longer strings) and the irreducible representation Π_u is a basis for 4p type inter-metallic bonds. This implies the M_e-M_i-M_e catalyst should be distinctly nonionic since these bonds have little or no s-character.

Different cooperative electron bonding may be inferred for the mutually degenerate representations $\Gamma(E_A)$ and $\Gamma(E_B)$. These individual representations, or linear combinations thereof, may be used to describe functions of the reactant and embryonic product. The full character table shows the central transition metal atom of the catalyst to be associated with the four carbon monoxide reactant molecules by means of sd^3 hybrid orbitals. While other hybrids such as sp^3, spd^2 or sp^2d may contribute to bonding their preferred geometries and probable bond energies indicate these make minor contributions. The essential molecular wave function of the catalyst will contain the atomic orbitals for the transition metal atoms and those atomic orbitals for the reactants that interact to create bonding. The 4s- and five 3d-orbitals of the central transition metal atom and the four sets of hybrid $2p_x$-, $2p_y$- and $2sp_z$-orbitals of the carbon monoxide ligands were combined in the molecular orbital expression of the complex[38]. The molecular wave function for the complex of figure 1 may be expressed as

$$\Psi = (\sqrt{35}/35)[\sqrt{2}\varphi_{4s}+\varphi_{3dxz}+\varphi_{3dyz}+\varphi_{3dxy}+\varphi_{3dz2}+\varphi_{3d(x2-y2)}] + (\sqrt{5}/10)[(\varphi^C_{2px}+\varphi^C_{2py}+\varphi^C_{2spz})^x$$
$$+(\sqrt{3}/3)(\varphi^O_{2px}+\varphi^O_{2py}+\varphi^O_{2spz})^x+(\varphi^C_{2px}+\varphi^C_{2py}+\varphi^C_{2spz})^y+(\sqrt{3}/3)(\varphi^O_{2px}+\varphi^O_{2py}+\varphi^O_{2spz})^y$$
$$+(\varphi^C_{2px}+\varphi^C_{2py}+\varphi^C_{2spz})^{-x}+(\sqrt{3}/3)(\varphi^O_{2px}+\varphi^O_{2py}+\varphi^O_{2spz})^{-x}+(\varphi^C_{2px}+\varphi^C_{2py}+\varphi^C_{2spz})^{-y}$$
$$+(\sqrt{3}/3)(\varphi^O_{2px}+\varphi^O_{2py}+\varphi^O_{2spz})^{-y}].$$

These M_e–$M_i$$(m\text{-}n)_4$–$M_e$ sd^3 symmetry constrained hybrid orbitals may be represented in an LCAO-MO approximation as two components conforming to the two-dimensional basis E of E_A and E_B as follows. That portion of Ψ in E_A that transforms according to the symmetry operation E is multiplied by the coefficient 2 (or by 1 when normalized) as $^\#\Psi_A = \Psi$ where the normalization constant N is 1. In similar fashion, that portion of Ψ in E_B that transforms according to the operation C_2 is multiplied by the coefficient -2 (or by 1 when normalized) as

$$^\#\Psi_B = N\{(\sqrt{35}/35)[\sqrt{2}\varphi_{4s}+\varphi_{3dz2}+\varphi_{3d(x2-y2)}]+(\sqrt{5}/10)[(\varphi^C_{2spz})^x+(\varphi^C_{2spz})^y+(\varphi^C_{2spz})^{-x}+(\varphi^C_{2spz})^{-y}$$
$$+(\sqrt{15}/30)[(\varphi^O_{2spz})^x+(\varphi^O_{2spz})^y+(\varphi^O_{2spz})^{-x}+(\varphi^O_{2spz})^{-y}]\}$$

for which the normalization constant N is $\sqrt{(21/11)}$. An analysis of the function $^\#\Psi_B$ shows that the C-O bonds all lie in the direction of the z-axis and the iron orbitals are oriented toward either side of the C and O atoms. It is apparent that the $^\#\Psi_B$ function represents the associated or catalyst-reactant π-complex. The $^\#\Psi_A$ wave function contains all of the C-O bonds, some lying along the x- and y-axes oriented toward the iron atoms. Iron contains all of its outer orbitals including the $3dxy$ and $3d(x^2 - y^2)$ orbitals oriented directly toward the C and O atoms. Thus, the $^\#\Psi_A$ function represents the σ-bonded molecule or embryonic product. During the instant of catalysis, when the initial chemical transformation caused by shifting of electrons from the transition metal to form M-C and M-O sigma bonds, this electron shift may be viewed as a barrier free transformation since these two electronic states are degenerate, or nearly so in the case of Jahn-Teller distortion[39].

There is an alternate but similar bonding arraignment possible for the polar reactant catalytic site represented by the formula M_e–$M_i$$(m\text{-}n)_4$–$M_e$. In this alternate geometry the four parallel C-O ligands have been bonded in alternating anti-parallel orientation such that the carbon end of the ligands are positioned in an up, down, up, down configuration relative to the vertical z-axis or Fe_3 string axis as shown in Figure 2. This form of the complex belongs to the D_{2h} point group[37,40].
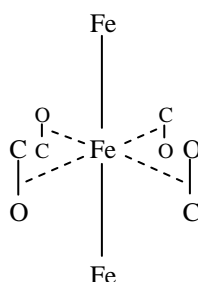
Figure 2. A Representation of Fe-Fe(*C-O*)$_4$-Fe In D_{2h} Symmetry.

Semi-empirical energy computations have been conducted[36,41] for the first row transition metal series in the M_e–$M_i$$(m$-$n)_4$–$M_e$ geometrical configuration of figure 2 where the V_3, Cr_3, Fe_3 and Ni_3 tetra-carbonyl complexes were shown to have lower energies than those same complexes computed having the standard C_{4v} geometry.

The propene-catalyst association, preceding Ziegler-Natta polymerization, may belong to a C_{3v} or a C_{4v} symmetry group, space permitting. The propenes associated with the catalytic site are most likely positioned with the pendant methyl groups lying away from the central z-axis. The bonds of monomeric propene are known to be σ-sp^2 hybrids with a π-$2pz$ configuration. For this reactant-catalyst association belonging to either a C_{3v} or a C_{4v} symmetry group the direct product $\Gamma(A_1)$ x $\Gamma(E)$ forms a basis for the wave functions during catalysis. The sd^3 hybrid on M (Fe in figure 2) has significant overlap with the
π-$2pz$ carbon orbitals and produces a similar wave function, as before.

Experimental evidence shows that the majority of polypropylene products form with head-to-tail bonding. This implies the propene ligands may be bonded in alternate anti-parallel orientation such that the methyl carbon end of a ligand is positioned in an up, down configuration relative to the M string axis or z-axis. For a more detailed description of continuing chain growth, as found in formation of polypropylene, refer to a thorough review by J. Boor[42]. It is of interest to note that catalysts active for propene oligomerization have been shown to be transition metal hydrides[42]. Here again, the reactant-catalyst association complex is doubly degenerate, and both the reactant complex and the embryonic product complex belong to identical classes of symmetry operations. This may also be viewed as a barrier free transformation since these two electronic states are degenerate or nearly so.

These symmetry requirements may be expressed in general terms as follows. Theorem 2: A catalyst, or host, and the guest reactants form a molecular association whose highest filled levels are degenerate. Theorem 3: Molecular bond symmetry is preserved such that the degeneracy of the highest filled level is not removed and barrier free electron transfer is facilitated. Theorem 2 relates to the symmetry associated with the metal-metal bonds and only those other nearest neighbor atoms associated with or directly bonded thereto. These atoms determine the symmetry of the host-guest molecular complex during catalysis. Vibration or re-arrangement of the other reactant or embryonic product atoms have inconsequential bearing on the symmetry related electronic configuration of the catalytic backbone itself. During the instant of catalysis, while the reactants proceed to form embryonic products, only the electrons shift but initially the atoms do not move in accord with the Franck-Condon principle[43]. They must await the relatively longer times required for molecular vibrations to occur for them to conform to their new locations. Such re-arrangements of the reactants in formation of products have been determined to pass through un-symmetrical geometrical configurations for some larger molecules. This has no bearing on theorem 3 since such motions occur after the catalytic cycle.

Reflection on the original definitions of catalysis presented in the introduction indicates that a new definition of catalysis is needed. The following definition is proposed: *catalysis is a barrier free transformation of one radiationless electronic configuration to another,* changing reactants to products.

Catalysts with associated non-polar reactants may be arrayed in the x-y plane, like the spokes of a wheel around the M_e–M_i–M_e or z-axis with one end of each ligand pointed toward the center[44]. Refer to figure 3. These molecular complexes belong to the D_{4h} symmetry group and the molecular wave function is best described by the two-dimensional irreducible representation E_g. This representation facilitates the central transition metal atom(s), -M_i- or –M_i-M_i-, of the catalyst as associated with the reactant oxygen molecule by means of sd^3 hybrid orbitals.

The spoke wheel geometric bond pattern for the $M_3$$(m$-$m)_4$ molecular complex, belonging to the D_{4h} symmetry group, has been verified by semi-empirical computations where the energies of these geometries were shown to lie lower than those of the D_{4h} symmetry group for the O-O ligands oriented co-parallel with the catalyst string axis. Here again group symmetry requires the bonding state be two-fold degenerate. Thus, an electron shift between the two degenerate levels may be viewed as a barrier free transformation.

It is instructive to review the physical observable or chemical effect of catalytic electron transfer that the symmetry constrained transformation of wave functions represents. Catalysis is shown in figures 4 and

5 where sp^2 – sd^3 π-type orbitals have been represented by dashed lines and sp^2 – sd^3 σ-type orbitals have been represented by solid lines. Reductive catalysis, such as hydrogenation of an alkene, formation of a
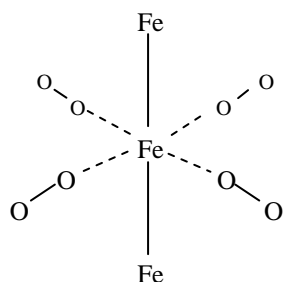
Figure 3. A Representation of $Fe_3(O\text{-}O)_4$ In D_{4h} Symmetry.

nitrile from hydrogen cyanide or a Fischer-Tropsch reductive carbonylation as presented in figure 4, indicates that a two electron transfer has been initiated causing Fe(0) to instantaneously become Fe(II) as shown,
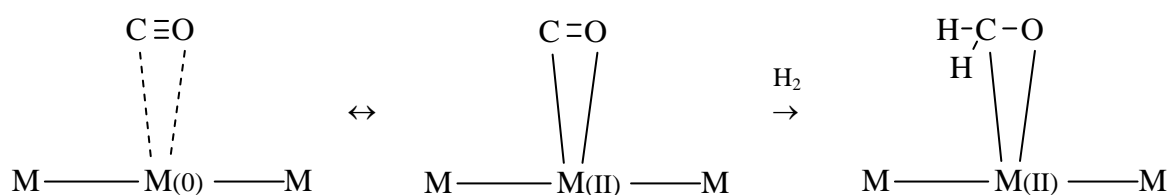
Figure 4. A Representation of Catalysis of $M_3(CO)$ To Form $M_3(CH_2O)$

The carbon monoxide reactant has been transformed into a formyl iron embryonic product[41]. As the embryonic product is released as neutral formaldehyde then Fe(II) immediately returns to Fe(0). The entire transformation is completed in time the order of a molecular vibration.

Oxidative catalyst's may initiate a one electron transfer that causes Fe(II) to briefly become Fe(III) as presented in figure 5 where half of a pair of reactions is shown and the full indicated reaction is represented by 4Fe(II)-Fe(II) + O_2 + $2H_2O$ → 4Fe(II)-Fe(III)OH. This later catalyst is used for ambient air oxidation
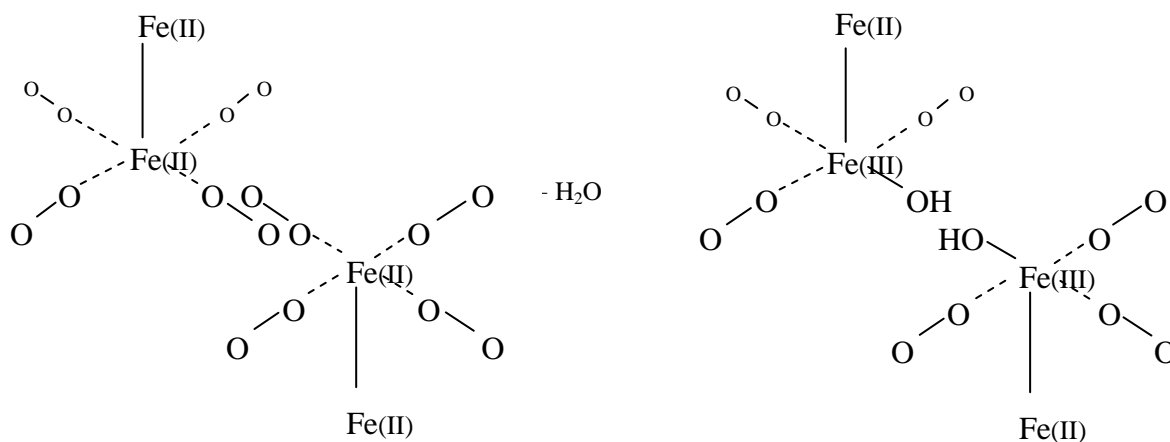
Figure 5. A Representation of Catalysis of $2M_2(O_2)_4$ To Form $2[M(OH)]_2(O_2)_3$

of alkanes resulting in formation of carbon monoxide and water by means of aldehydes and unsaturated alcohol intermediates[45]. Such one electron catalytic transformations are similar to free radical reactions however, as soon as an oxidative attack of a hydrocarbon reactant occurs, then the catalytic Fe(III) immediately returns to Fe(II) making possible observable unpaired electron character short lived.

IV. Energy of Selected Catalyst Reactant Complexes

Single cycle (non-iterative) Hartree-Fock (H-F) energies have been computed for two model catalysts. Symmetry constrained one-electron hydrogen-like wave functions were used[46-48]in construction of many electron Slater determinants, to confirm that the catalyst reactant complex bond energies lie in the anticipated -5 to -60 kcal/mol range. Symmetry constrained functions may be considered to be optimized such that iteration of H-F energies is not necessary. First the bond energy was computed for the specific polar reactants, carbon monoxide, complexed with an iron atom of a Fischer-Tropsch catalyst. A nine-atom model $Fe(C-O)_4$ was considered in which the associated carbon monoxide molecules were assumed to be bonded symmetrically as belonging to the C_{4v} point group with a single, zero valent iron atom. A bond distance of 209.5 pm was selected for the Fe-C and Fe-O bonds based on averages of x-ray crystallographic measurements[49], which ranged from an average of 187 pm to an average of 224 pm, and was similar in

value to a related computation[50]. A bond distance of 120.5 pm was selected for the C-O bond based on the averages of x-ray crystallographic measurements[51,52]. Molecular orbital bond energies were computed using the Hartree-Fock formalism for a closed shell function[53,54]. The symmetry determined functions, $^{\#}\Psi$, were considered to be essentially equivalent to the result of an SCF computed function derived from the iterative Roothan-Hall equations[55],

$$\sum_{\nu=1}^{N} (F_{\mu\nu} - \varepsilon_i S_{\mu\nu})\, c_{\nu i} = 0 \quad \text{for} \quad \mu = 1, 2, ..., N$$

where the Fock matrix is defined as

$$F_{\mu\nu} = H_{\mu\nu}^{core} + \sum_{\lambda=1}^{N}\sum_{\sigma=1}^{N} P_{\lambda\sigma}\,[(\mu\nu|\lambda\sigma) - \tfrac{1}{2}(\mu\lambda|\nu\sigma)]$$

and the density matrix is

$$P_{\mu\nu} = 2\sum_{i=1}^{occ.} c_{\lambda i}^{*} c_{\sigma i}$$

Each entry in the determinant was composed of a linear combination of orthonormal hydrogen-like atomic functions[46] as shown in equations presented previously. Under these conditions the density matrix, P, may be simplified to

$$P_{\mu\mu} = 2c_{\mu}^{*}c_{\mu} \quad \text{and} \quad S_{\mu\nu} = \delta_{\mu\nu}$$

for which S represents the overlap matrix. Further, the Fock matrix may be reduced to

$$F_{\mu\mu} = (1/2)P_{\mu\mu}(\mu\mu|\mu\mu)$$

for which $(\mu\mu|\mu\mu)$ represents the diagonal two electron repulsion integrals. All core electrons were neglected as their energy contributions may be considered to be an additive constant. A non-iterative (single cycle) bond energy of -2.5269 eV (-58 kcal/mol, -244 kJ/mol) was computed for the associated complex.

The individual iron penta-carbonyl dissociation energies were determined by a semi-empirical method in which the computed $Fe(CO)_4$ energy was referenced to the computed Hartree-Fock value of -58 kcal/mol. A dissociation bond energy of $Fe(CO)_3$ = -44 kcal/mol was computed. The $Fe(CO)_3$ = -44 kcal/mol value compares with an experimental dissociation energy of -42 kcal/mol[56] and is in fair agreement with more extensive computational values of -46.5 kcal/mol[57] and -45.7 kcal/mol[58] thus lending support to the $Fe(CO)_4$ value of -2.5269 eV (-58 kcal/mol).

In addition, a nine-atom model was considered for associated non-polar oxygen molecules bonded symmetrically in a spoke wheel pattern with a single iron(II) ion of the $Fe(II)(O-O)_4$ complex. A Fe-O bond distance of 192.7 pm was selected which is slightly longer than 190 pm for aquocobaltamine[59] and similar to copper(II)-oxygen ligand bond distances of 193 pm[60,61]. The selected O-O bond distance of 125.0 pm is longer than the 120.8 pm bond for oxygen in the gas state[59] and significantly shorter than the 141.2 pm oxygen-oxygen bond length reported[61] for a peroxide bond. Molecular bond energies were computed for $Fe(II)(O-O)_4$ using the

Hartree-Fock formalism for a closed shell function[53] where a similar symmetry constrained many electron determinant was chosen for four oxygen molecules associated with an iron ion and was expressed as before. A non-iterative (single cycle) bond energy of -1.5198 eV

(-35 kcal/mol, -147 kJ/mol) was computed. The bond energy has been related to the individual iron oxygen dissociation energies by a semi-empirical method in which the $Fe(II)_2(O_2)_4$ energy was referenced to the Hartree-Fock value of -35 kcal/mol. A molecular dissociation energy for $Fe(II)_2(O_2)_3$ = -41 kcal/mol was computed. These computations demonstrate that both catalyst complexes have bond energies in the anticipated -5 to -60 kcal/mol range.

V. Transition Probability of a Catalytic Complex

Catalysis has often been discussed in terms of a kinetic transition state theory[62] model where molecules are treated as a set of atoms connected together by mechanical springs and assigned classical rates of vibration. Passage of such a reactant over the energy barrier is considered as motion in only one degree of freedom and motion along this reaction coordinate is assumed[63] to be independent of all other motions. Thus, this model assumed that the energy of this reaction coordinate to be separable from that of other coordinates. When the rate constant is considered in terms of the Arrhenius equation, the activation energy has been represented by an exponential factor that may be described in terms of thermodynamic functions.

The quantum energy state of a reactant-catalyst complex is described by its wave function representing the entire molecule including electronic, vibrational and rotational states rather than a single coordinate. These energy states are considered separable according to the Frank-Condon principle. An electronic state of a molecule may lose a quantum of energy during a transition to a lower allowed energy state[64]. Electronic transitions are discussed in terms of transition probabilities or the transition moment between reactant state r and embryonic product state p. Instead of considering a transition state to follow a classical reaction coordinate, a transition state is treated here as a change in electronic state. Catalysis may be represented as a change in electronic states followed by a shift in vibrational states driven by the difference between the thermodynamic energy of the reactant and the product.

A measure of the efficiency of a catalyst may be determined by its transition probability, just as the intensity of a spectral line is associated with the transition probability of one allowed state to another. An electronic transition, such as a stimulated emission of radiation from a system of atoms or molecules, is represented by an electric dipole moment[65]. A dipole moment is the sum of electric moments from each component in the system as given by $\mu = \Sigma_i r_i e_i$ for which the quadrapole and higher moment terms are neglected as small compared to the dipole. Here r_i represents the length of a local dipole and e_i is its electronic charge. The transition probability of a catalyzed system of reactant molecules is expected to be adequately described in terms of the same electric dipole moment except catalysis would result in the expectation of a radiationless transition[8] to a new electronic configuration. Such an electronic transition occurring between the reactant Ψ_r and embryonic product Ψ_p states may be expressed in terms of the transition moment m_μ as given by the expression $m_\mu = \int \Psi_r^* \mu \Psi_p d\tau$ for which μ is the amplitude of the induced dipole moment along the symmetry axis. Here the transition moment is a measure of the tendency of this molecular system to initiate an electronic transition and the condition that an electronic transition be allowed is that at least one value of $\Sigma_i r_i e_i$, or in vector form $e \bullet r$, be nonzero for

$$m_\mu = \int \Psi_r^* e \Sigma_i r_i \Psi_p d\tau \ .$$

The integral m_μ will be nonzero provided the direct product of the irreducible representations of the functions Ψ_r and Ψ_p contains the requirement of the symmetric irreducible representations Γ_A as found, for example, in the character table for the C_{4v} symmetry group. Einstein's transition probabilities[66] are seen to be wholly applicable for describing the electronic transition of molecular catalysis recognizing the energy term, $\hbar\omega$, representing the energy of catalysis is the energy required for the catalyst to temporarily achieve an excited state necessary to cause an electron transfer to a reactant.

Catalytic transition rates may be derived more directly from a form of Fermi's golden rule[51] of time-dependent perturbation theory,

$$w = (2\pi/\hbar)[\int \Psi_r (e \bullet r)\Psi_p d\tau]^2 \ \rho(E_p),$$

where $e \bullet r$ is the perturbation potential that couples eigenstates of the unperturbed Hamiltonian causing transitions, which are anticipated to be of highest probability between degenerate states ($\Delta E \sim 0$), and $\rho(E_s)$ is the number density of unperturbed energy states[68]. Spontaneous, radiationless catalytic transitions proceed by

means of an electric dipole perturbation originating in a narrow frequency spectrum σ(ω) of those states. By integrating over a narrow frequency band rather than the number density of states the transition probability resulting from an electric dipole perturbation becomes

$$\int\sigma(\omega)d\omega = 4\pi^2\alpha'\omega[\int\Psi_r(e \bullet r)\Psi_p d\tau]^2$$

where σ(ω) represents the narrow catalysis frequency (energy) distribution, *e* represents a unit vector of the catalyst, *r* is the vector representing the dipole perturbation and α' is the fine structure constant representing a collection of constants. Spontaneous catalysis from a perturbed state may occur once so it is necessary to consider the time rate of change of the transition probability, w, in an increment of space, dΩ, directed between the catalyst and a reactant producing a total transition probability of

$$\Sigma w = (1/2\pi)\int(\omega/2\pi c)^2 d\Omega \int\sigma(\omega)d\omega.$$

Direct substitution of the ∫σ(ω)dω equation into the Σw equation produces

$$\Sigma w = \int(\alpha\omega^3/2\pi c^2)[\int\Psi_r(e \bullet r)\Psi_p d\tau]^2 d\Omega.$$

Integration over an increment of space can be performed recognizing that the vector directions *e* and *r* are related through a solid angle θ so dΩ = cos²θdθ and

$$\Sigma w = \int(\alpha\omega^3/2\pi c^2) \cos^2\theta \ [\int\Psi_r(e \bullet r)\Psi_p d\tau]^2 d\theta$$
$$= (4\alpha\omega^3/3c^2)[\int\Psi_r \mathbf{r}\Psi_p d\tau]^2 .$$

Thus, the total transition rate per unit time is a product of the energy times the transition probability as

$$I = \hbar\omega\Sigma w$$
$$= (e^2\omega^4/3\pi\varepsilon_0 c)[\int\Psi_r \mathbf{r}\Psi_p d\tau]^2 .$$

This is an expression of the catalytic transition probability computed based on its transition moment.

Computation of the transition moment can be conducted directly for a specific Fischer-Tropsch (F-T) catalyst complex Fe(*C-O*)₄ (neglecting the second and third metal atoms for simplicity). The transition moment was computed using orthonormalized hydrogen-like one-electron wave functions, as given by Pauling & Wilson[46], for the 4s, 3d and 2p orbitals for ease of computation as

$$m_\mu = \int{}^{\#}\Psi_B \ \mathbf{r} \ {}^{\#}\Psi_A d\tau$$

$$= \int_0^\infty \int_0^\pi \int_0^{2\pi} {}^{\#}\Psi_B \ \mathbf{r} \ {}^{\#}\Psi_A \ r^2\sin\theta \ d\varphi \ d\theta \ dr$$

These functions are presented in terms of the variable ρ = (2Z/na₀)r for which Z is the atomic charge of the nucleus, n is the principle quantum number and a₀ is the Bohr radius given as a₀ = h²/4π²ue² for which u is the reduced mass for a transition moment expressed as

$$m_\mu = (na_0/2Z)^4 \int_0^\infty \int_0^\pi \int_0^{2\pi} {}^{\#}\Psi_B\rho \ {}^{\#}\Psi_A \ \rho^2\sin\theta \ d\varphi \ d\theta \ d\rho$$

All integrals were evaluated and the result of computation is $m_\mu = 0.243$. The value of this transition moment is significant (in the region of unity) indicating the tendency toward catalytic transition of the specific F-T catalyst complex, Fe(*C-O*)₄, to products is quite probable. The transition probability is not to be construed to indicate oxidation or reduction since the time of a catalytically stimulated transition is expected to be less than the time of

a molecular vibration ($< 10^{-12}$ second) following which the shifted electrons return to the original electronic configuration of the catalyst leaving products in place of the reactants. Thus, all atoms remain in their original positions until the electronic transformation (catalysis) is complete, as indicated in the propene dimerization in figure 6 of Appendix I. Following this the atoms shift slightly or vibrate to their new locations.

VI. Stabilization of the Catalyst Against Permanent Oxidation

A transition metal atom whose outer shell is not filled by electrons (has not achieved an inert gas configuration) may be subject to permanent oxidation by perturbing species. During a catalytic transformation when an electron shift leaves the active transition metal in a temporary electron deficient state it becomes subject to permanent oxidation. A potential barrier necessarily needs to be put into place to protect the active site by and from its nearest neighbor atoms. Enzymes appear to be designed with these large molecular shields surrounding and protecting their core catalytic transition metal sites. The vulnerable internal atom or active site M_i of a symmetric tri-metal catalyst M_e-M_i-M_e may be protected by bonding relatively electron rich atoms M_e adjacent to it to assure immediate re-establishment of a reduced state. The external atoms or groups, M_e, must possess the same or greater electronegativity as M_i to fulfill this requirement. Elements of the first transition metal series increase in electronegativity[54] with increasing atomic number. For example, if Fe is the M_i atom then only Fe, Co, Ni or Cu, those atoms with the same or higher electronegativity can be effective M_e atoms in this series of elements while the atoms Ti, V, Cr and Mn would not be acceptable for stabilization of Fe. These adjacent atoms of lower electronegativity do not negate a catalyst's activity but the life of such a catalyst is anticipated to be short as M_i may tend to oxidize to satisfy the electronegative deficiency of M_e. This stability requirement distinctly limits the number of symmetric tri-atomic catalyst clusters like M_e-M_i-M_e for the first transition metal series to 41 strings, from Ti through Cu, refer to Table 4. Similar numbers of tri-atomic strings can be generated for the second and third transition metal series, refer to Tables 5 and 6. A larger number of symmetric tri-atomic strings can be generated provided there is inter-series mixing of the elements. Even catalysts similar to M_e-M_i-M_e' may be allowed, for M_e not the same as M_e', provided the effect on symmetry constraints is minimal.

Table 4. Allowed Bi-metal And Symmetric Tri-metal First Row Transition Metal Linear Catalysts

Ti-Ti	Mn-Ti	Co-Cr	Ni-Ti	Ni-Cu-Ni	Ni-Fe-Ni	V-Cr-V	Ni-V-Ni
V-V	Fe-Fe	Co-V	Cu-Cu	Cu-Cu-Cu	Cu-Fe-Cu	Cr-Cr-Cr	Cu-V-Cu
V-Ti	Fe-Mn	Co-Ti	Cu-Ni	Co-Ni-Co	Ti-Mn-Ti	Fe-Cr-Fe	Ti-Ti-Ti
Cr-Cr	Fe-Cr	Ni-Ni	Cu-Co	Ni-Ni-Ni	V-Mn-V	Co-Cr-Co	V-Ti-V
Cr-V	Fe-V	Ni-Co	Cu-Fe	Cu-Ni-Cu	Cr-Mn-Cr	Ni-Cr-Ni	Cr-Ti-Cr
Cr-Ti	Fe-Ti	Ni-Fe	Cu-Mn	Co-Co-Co	Mn-Mn-Mn	Cu-Cr-Cu	Mn-Ti-Mn
Mn-Mn	Co-Co	Ni-Mn	Cu-Cr	Ni-Co-Ni	Fe-Mn-Fe	V-V-V	Fe-Ti-Fe
Mn-Cr	Co-Fe	Ni-Cr	Cu-V	Cu-Co-Cu	Co-Mn-Co	Cr-V-Cr	Co-Ti-Co
Mn-V	Co-Mn	Ni-V	Cu-Ti	Fe-Fe-Fe	Ni-Mn-Ni	Fe-V-Fe	Ni-Ti-Ni
			Co-Cu-Co	Co-Fe-Co	Cu-Mn-Cu	Co-V-Co	Cu-Ti-Cu

Table 5. Bi And Symmetric Tri-metal Second Row Transition Metal Linear Catalysts

Zr-Zr	Tc-Zr	Rh-Mo	Pd-Zr	Tc-Ag-Tc	Pd-Rh-Pd	Tc-Mo-Tc	Pd-Nb-Pd
Nb-Nb	Ru-Ru	Rh-Nb	Ag-Ag	Ru-Ag-Ru	Ru-Ru-Ru	Ru-Mo-Ru	Ag-Nb-Ag
Nb-Zr	Ru-Tc	Rh-Zr	Ag-Pd	Rh-Ag-Rh	Rh-Ru-Rh	Rh-Mo-Rh	Zr-Zr-Zr
Mo-Mo	Ru-Mo	Pd-Pd	Ag-Rh	Pd-Ag-Pd	Pd-Ru-Pd	Pd-Mo-Pd	Nb-Zr-Nb
Mo-Nb	Ru-Nb	Pd-Rh	Ag-Ru	Ag-Ag-Ag	Tc-Tc-Tc	Ag-Mo-Ag	Mo-Zr-Mo
Mo-Zr	Ru-Zr	Pd-Ru	Ag-Tc	Ru-Pd-Ru	Ru-Tc-Ru	Nb-Nb-Nb	Tc-Zr-Tc
Tc-Tc	Rh-Rh	Pd-Tc	Ag-Mo	Rh-Pd-Rh	Rh-Tc-Rh	Mo-Nb-Mo	Ru-Zr-Ru
Tc-Mo	Rh-Ru	Pd-Mo	Ag-Nb	Pd-Pd-Pd	Pd-Tc-Pd	Tc-Nb-Tc	Rh-Zr-Rh
Tc-Nb	Rh-Tc	Pd-Nb	Ag-Zr	Ru-Rh-Ru	Ag-Tc-Ag	Ru-Nb-Ru	Pd-Zr-Pd
				Rh-Rh-Rh	Mo-Mo-Mo	Rh-Nb-Rh	Ag-Zr-Ag

Table 6. Bi And Symmetric Tri-metal Third Row Transition Metal Linear Catalysts

Hf-Hf	Re-Hf	Ir-W	Pt-Hf	Au-Au-Au	Ir-Os-Ir	Os-W-Os	Au-Ta-Au
Ta-Ta	Os-Os	Ir-Ta	Au-Au	Os-Pt-Os	Pt-Os-Pt	Ir-W-Ir	Hf-Hf-Hf
Ta-Hf	Os-Re	Ir-Hf	Au-Pt	Ir-Pt-Ir	Au-Os-Au	Pt-W-Pt	Ta-Hf-Ta
W-W	Os-W	Pt-Pt	Au-Ir	Pt-Pt-Pt	Re-Re-Re	Au-W-Au	W-Hf-W
W-Ta	Os-Ta	Pt-Ir	Au-Os	Au-Pt-Au	Os-Re-Os	Ta-Ta-Ta	Re-Hf-Re
W-Hf	Os-Hf	Pt-Os	Au-Re	Os-Ir-Os	Ir-Re-Ir	W-Ta-W	Os-Hf-Os
Re-Re	Ir-Ir	Pt-Re	Au-W	Ir-Ir-Ir	Pt-Re-Pt	Re-Ta-Re	Ir-Hf-Ir
Re-W	Ir-Os	Pt-W	Au-Ta	Pt-Ir-Pt	Au-Re-Au	Os-Ta-Os	Pt-Hf-Pt
Re-Ta	Ir-Re	Pt-Ta	Au-Hf	Au-Ir-Au	W-W-W	Ir-Ta-Ir	Au-Hf-Au
				Os-Os-Os	Re-W-Re	Pt-Ta-Pt	

Pauling electronegativities[69-71] for the first-row transition metal series atoms increase with increasing atomic number from approximately 1.2 for Sc to 1.7 for Zn. The approximate values taken from figure 2.4 of reference[70] are χ_{Ti}=1.5, χ_V=1.6, χ_{Cr}=1.6, χ_{Mn}=1.5, χ_{Fe}=1.8, χ_{Co}=1.9, χ_{Ni}=1.9 and χ_{Cu}=1.9. While the χ values in general increase with increasing atomic number, the value of χ_{Mn} falls below the linear trend line. Common anions also have electronegativity values higher than the transition metals, namely χ_F=4.0, χ_{Cl}=3.0, χ_{Br}=2.8, χ_I=2.5, χ_O=3.5, χ_S=2.5, χ_N=3.0, χ_P=2.1, χ_{NO3}=3.3, χ_{SO4}=3.3 and χ_{PO4}=3.2. Thus, a compound, which employs these anions as the external groups M_e, such as the chlorine atoms in the bent geometric configuration of $MnCl_2$, may be relatively stable and become an active catalyst during that portion of time its vibrational motion passes through a linear configuration.

The electronegativity values dictate which atoms can be placed at the external Y position in a catalyst molecule represented by Y-M-Y such that $\chi_Y > \chi_M$. This concept may be represented in general as follows. Theorem 4: The active catalytic site exhibits low electron density yet is buffered against permanent oxidation by adjacent electronegative groups. Theorem 4 describes the relative protection of the active transition metal site during that instant when it lends one or more electrons to the complex to initiate

a catalytic transformation. Should the active site be left unprotected the relatively more electronegative reactants may tend to react directly with the catalyst producing an unwanted product, thus terminating the activity of the catalyst.

Protection of the active site from oxidation by nearest neighbor atoms has been addressed but the catalyst may still be subject to oxidative attack from outside influences. A catalyst may be further insulated through saturation of its outer or coordination shell to attain a noble gas configuration. This is known as the rule of 18 for a first-row transition metal or 32 for a second and third row transition metal atom[72]. By adding the number of valence electrons associated with the catalytic transition metal atom, compliance with the rule of 18 is determined for the active site. Should the total number of electrons be less than 18 the coordination shell can be filled through donation of non-bonding electrons from associated ligands. Thus, the rule of 18 (or 32) can be satisfied for a constructed or designed catalyst by addition of ligands with non-bonding electrons to preserve its stability.

VII. Molecular Catalyst Design with Applications

The concepts of catalysis, as discussed in the previous sections, forms a basis for design of molecular catalysts and their precursors for known chemical reactions through simple computational methods as organized in the following six steps. (Step 1) Express a molecular mechanism for the specific reaction that is to be catalyzed by employing sufficient complexed reactants to satisfy the degeneracy requirement of Theorem 2. (Step 2) Select an active metal site, M, and form a catalytic backbone structure or string (Theorem 1), Y-M-Y, as taught or by using tables 4, 5 or 6 (Theorem 4). Note: Catalysts of the form

Y-M-Y or M-M-M are assumed in the selection process, however, other catalysts that conform to the selection rules are also possible. (Step 3) Compute an associated bonding energy for reactants (guests) associated with their catalytic metal site (host) where the catalyst is in a two or three metal atom string such as M_2, M_3 or Y-M-Y to verify that the degenerate species lies in the -5 to -60 kcal/mol energy range. (Step 4) Identify the valence-state of the highest filled energy level that is doubly or triply degenerate to comply with Theorem 3. (Step 5) If the valence of M is greater than zero choose a chemically compatible anion (or anions) that exhibits greater electronegativity than the metal to complete the coordination shell. (Step 6) Determine if the outer coordination shell of the host-guest complex conforms to the rule of 18 for M being a first-row transition metal or 32 if a second or third row transition metal atom[72]. If the rule of 18 (or 32) is met, then a catalyst has been designed. If the rule of 18 (or 32) has not been met, then compatible electron donating ligands are to be added in formation of a catalyst precursor to attain agreement with the rule of 18 (or 32). Should such ligands be added a new bonding energy of the complex may be computed. The experimentalist should anticipate that one or more of the associated ligands of a precursor may be subsequently displaced by a reactant in formation of the active catalyst.

Design of an optimum catalyst, for a specific reactant, follows the same rules except the computations are to be performed for each member of a transition metal series to identify any preferred element. Not all catalysts are expected to perform well at room temperature and some may require elevated temperatures due to thermodynamic limitations of the reaction.

Two examples of the catalyst selection process are presented here. Both these and related catalyst families have been prepared in the laboratory and all these catalysts have proven to be active at room temperature and above.

Example 1. A Fischer-Tropsch catalyst[41], such as $Co(HCN)_2 \bullet Fe(HCN)_2 \bullet Co(HCN)_2$, can be selected by this process. A C_1 insertion mechanism was assumed and the guest reactant molecules, hydrogen cyanide or carbon monoxide, were identified (Step 1). Iron (Fe) was selected as the catalytic site[36] for the

Co-Fe-Co backbone or string for which the electronegativity value of Co is slightly greater than that of Fe (Step 2) and a bonding energy to associated carbon monoxide reactants of -58 kcal/mol (-243 kJ/mol) was computed, refer to section VII (Step 3). Since $M_3(CO)_4$ bond energies were negative or close to zero for most elements in the first transition metal series then the complexes, except those containing Ti and Ni, were anticipated to be catalytic. The first valence state for which the energy values were doubly degenerate

was zero (Step 4) so that no anions were required (Step 5). The rule of 18 was met as neutral iron contributed six 3d-electrons and two 4s-electrons, each hydrogen cyanide (or carbon monoxide) associated with the iron atom contributed two 2p-electrons and each cobalt atom contributed the remaining

3d-electrons for a total valence set of 18 electrons (Step 6). An approximate associated bond energy for the reactant CO associated with the catalyst was computed by a semi-empirical method, referenced as described in the previous section, of -14 kcal/mol (-59 kJ/mol). It was decided the catalyst could be made by reducing $Co(CN)_2 \bullet Fe(CN)_2 \bullet Co(CN)_2$ in hydrogen rich synthesis gas. Alternatively, this same process also selected the more common $Fe(HCN)_2 - Fe(HCN)_2 - Fe(HCN)_2$ or Fe_3 type catalyst. Refer to the article entitled, A Molecular Mechanism for Fischer-Tropsch Catalysis[41], for experimental results wherein a range of liquid hydrocarbons were produced for the Co-Fe-Co catalyst and waxy hydrocarbons were produced for the Fe-Fe-Fe catalyst.

Example 2. An ambient temperature air oxidation catalyst[45] $Fe(CN)_2L \bullet Fe(CN)_2L$, precursor to formation of $Fe(CN)_2L \bullet Fe(CN)_2OH + L$ for L being $K_3Cu(CN)_4$ and other ligands, was selected in a similar fashion for oxidation of aliphatic hydrocarbons. An acceptable oxidation mechanism, involving dual iron strings of two iron atoms per string, was established for O_2 in the presence of water (Step 1). Iron (Fe), the selected catalytic site[73], as part of an Fe-Fe string (Step 2) and an approximate bonding energy of -35 kcal/mol

(-146 kJ/mol), was computed (Step 3). Computations for each element of the first row transition metal series indicated all complexes, except for those containing Ti, V or Cr, were anticipated to be catalytic. The first valence state for which the energy values were two-fold degenerate was 2+ (Step 4). Pairs of cyanide and chloride ions were chosen as chemically compatible with the Fe in formation of a catalyst precursor (Step 5). Preliminary donated electron count showed the rule of 18 was not met so compatible ligands of the form $K_3Cu(CN)_4$ were added to complete the coordination shell. In this case the catalytic iron ion contributed six 3d-electrons, each cyanide ion contributed two 2p-electrons, two of the complexed cyanide ligands contributed two electrons each and the adjacent transition metal contributed four

3d-electrons for a total of 18 electrons (Step 6). Replacement of the ligands, L, by similar groups and also by the oxalate anion in the $Fe(CN)_2L \bullet Fe(CN)_2L$ catalyst also produced active catalysts. An approximate associated bonding energy of -16 kcal/mol (-67 kJ/mol) was computed for the catalyst-oxygen association with the ligands present. The catalyst oxidatively destroyed 1.4 grams of n-decane in water at 16°C in air in 5 hours. Refer to the following paragraph and the article entitled, Catalytic Air Oxidation of Ambient Temperature Hydrocarbons[45] for selected experimental results.

A significant number of catalysts have been prepared in the laboratory, based on this work, for use in Fischer-Tropsch conversions[41]. In addition, several catalysts were prepared and tested for ambient temperature air oxidation of hydrocarbons[45] including hexanes, n-decane, gasoline, diesel fuel and jet fuel in water. The Fischer-Tropsch catalyst $Co(HCN)_2 \bullet Fe(HCN)_2 \bullet Co(HCN)_2$ was responsible for direct formation of liquid hydrocarbons in the C_8 to C_{22} range at room temperature. The GC-MS and FTIR molecular spectra did show the products to be linear aliphatic hydrocarbons. Direct mass spectroscopic measurements were recorded for products formed in the first 30 seconds and the first 5 minutes of reaction at room temperature. This afforded the opportunity to identify the range of products and a molecular mechanism[41] was proposed for the Fischer-Tropsch catalytic reaction forming aliphatic hydrocarbons and the other products. An $Fe(HCN)_2 \bullet Fe(HCN)_2 \bullet Fe(HCN)_2$ catalyst formed the usual waxy aliphatic hydrocarbons.

In addition, five different oxidation catalysts of the form $Fe(CN)_2L \bullet Fe(CN)_2L$, for L being $K_3Cu(CN)_4$ and related ligands, were prepared for ambient air oxidative destruction of 20 mg/kg gasoline, 100 mg/kg diesel fuel and 200 mg/kg hexanes in water in 15 to 30 minutes[45] as well as for 14,400 mg/kg n-decane in water in 5 hours. Isolated hydrocarbon residues were shown to be primarily aldehydes with some unsaturated alcohols, while the ultimate products were carbon monoxide and water. All prepared catalysts were tested and found to be active for their respective reaction chemistries. Other applications include a theoretical computation of the first five reaction steps demonstrating the chromium silicate polymerization mechanism[74] and a nickel(I) ethylene polymerization reaction mechanism[75].

These applications of the Concepts of Catalysis served to confirm their functionality and established an overview of catalytic mechanisms. Possibly these principles will lead to an understanding of the function of enzymes, specifically how the methane mono-oxygenase enzyme[17,18] air oxidizes methane at ambient temperature.

VIII. Conclusions

The required linear configuration for a catalyst's essential geometry or backbone has been established and the symmetry restricted degenerate states have been indicated to be necessary for catalysis. Simultaneous existence of an associated reactant and an embryonic product on the linear or string catalyst rests on the fundamental requirement for degenerate electronic states. This leads to a new definition of catalysis, namely, catalysis is a barrier free transformation of one electronic configuration to another, changing reactants to products. Since enzymes perform catalytic functions they may also act as natural, symmetry-based catalysts.

A stepwise process for catalyst design at the molecular level has been developed through application of these concepts. Specific examples of catalysts prepared, without prior thermal conditioning, for air oxidative destruction of aliphatic hydrocarbons and Fischer-Tropsch catalytic conversion of synthesis gas to liquid hydrocarbons at room temperature and above demonstrate the applicability of the catalyst concepts. It is hoped that this work will add to the existing body of catalysis knowledge, shed light on the mechanism of enzymatic reactions and give industry new opportunities for catalytic process development, and expanded growth in the future.

References

[1].   Borman S. *Chem. & Eng. News* **2004** *82 (8)*, 35.
[2].   Pauling, L. *General Chemistry*, W.H. Freeman & Company: San Francisco, **1959**, 2nd ed., p115.
[3].   Cotton, F. A.; Wilkinson, G. *Advanced Inorganic Chemistry*, John Wiley & Sons: New York, **1980**, 4th ed., p1265.
[4].   Lewis, G. N.; Randall, M.; Pitzer, K. S.; Brewer, L. *Thermodynamics*, McGraw-Hill Book Company, Inc.: New York, 2nd ed., **1961**, p 273f.
[5].   Benson, S. W. *The Foundations of Chemical Kinetics*, McGraw-Hill Book Company: New York, **1960**, p 21).
[6].   This is not quantum tunneling since the reactant mass is much greater than that of a proton.
[7].   Electronic transitions may result in emission of radiation or be radiationless where the emitted energy is immediately transferred to a symmetry allowed level or set of molecular bonds.
[8].   Hehre, W. J.; Radom, L.; Schleyer, P. v. R.; Pople, J. A. *Ab Initio Molecular Orbital Theory* John Wiley & Sons: New York, **1986**, p12.
[9].   Lide, D. R. *CRC Handbook of Chemistry and Physics* CRC Press, Inc.: Boca Raton, Florida, **1997**, Sect. 9, p 63.
[10].   Margenau, H.; Murphy, G.M. *The Mathematics of Physics and Chemistry* D. Van Nostrand Co.:
[11].   New York, **1962**, p 338.
[12].   Margenau, H.; Murphy, G.M. *op cit*, p 330.
[13].   Margenau, H.; Murphy, G.M. *op cit*, p 331.
[14].   Tolman, W. B.; Que, Jr., L.; Halfen, J. A.; Wilkinson, E. C.; Mahapatra, S. Science **1996** *271*, 1397.
[15].   Lipscomb, J. D.; Que, Jr., L.; Shu, L.; Neshelm, J. Science **1997** *275*, 515.
[16].   Cambillau, C.; Brown, K. *Nat. Struc. Biol.* **2000** *7*, 191.
[17].   Woodland, M.P.; Patel, D.S.; Cammack, R.; Dalton, H. *Biochim. Biophys. Acta* **1986** *873*, 237.
[18].   Rosenzweig, A.C.; Frederick, C.A.; Lippard, S.J.; Nordlund, P. *Crystal Structure of a Bacterial non-haem Iron Hydroxylase that Catalyses the Biological Oxidation of Methane, Nature* **1993** *366*, 537-43.
[19].   Hartwig, J.F.; Stambuli, J.P.; Ryoichi, X.; Kuwano, Y. *Angew. Chem. Int. Ed.* **2002** *41*, 4746.
[20].   Dwyer, D. J.; Somorjai, G. A. *J. Catal.* **1978** *52 (2)*, 291-301.
[21].   Biloen, P.; Helle, J. N.; Sachtler, W. M. H. *J. Catal.* **1979** *58 (1)*, 95-107.
[22].   Masters; Van Doorn, U.K. Patent Application **1975** No. 40322-75.
[23].   Beier; Muetterties, *J. Am. Chem. Soc.* **1976** *98*, 1296.
[24].   Muetterties, *Bull. Chem. Soc. Belg.* **1975** *84*, 959.
[25].   Brenner; Hucul, *J. Am. Chem. Soc.* **1980** *102*, 2484.
[26].   Reit; Copperwaite; Hutchings, *Chem. Soc. Faraday Trans.* **1987** *83*, 2963.
[27].   Colley; Copperwaite; Hutchings; Terblanche; Thackerary *Nature* **1989** *339*, 129-30.
[28].   Donnelly, T. J.; Satterfield, C. N. *Appl. Catal.* **1989** *52*, 93.
[29].   Donnelly, T. J.; Satterfield, C. N. *Department of Energy Contract No. DE-AC22-85-PC80015.*
[30].   Zarochak, M. F.; MacDonald, M. A.; Rao, V. U. S. *Stability and Selectivity of Potassium Promoted Iron Catalyst in Slurry Fischer-Tropsch Synthesis*, 12th Annual Conference on Fuel Sciences, Palo Alto, CA, **1987** May 13-14.
[31].   Chen, Guangun; Zou, Ningmu; Chen, Bo; Sambur, Justin B.; Choudhary, Eric; Chen, Peng *ACS Cent. Sci.* **2017** *3,* 1189; DOI: 10.1021/acscentsci.7b00377.
[32].   F.H. Jardine, et al., *J. Chem. Soc.*, **1966** A, 1711.
[33].   Morimoto, T.; Ogata, Y. *J. Chem. Soc.,* **1967** *B 12*, 1353.
[34].   Benson, S. W. *The Foundations of Chemical Kinetics*, McGraw-Hill Book Company: New York, **1960**, pp 122-127, 247.
[35].   Bohm, D. *Quantum Theory*, Prentice-Hall, Inc., Englewood Cliffs, NJ, **1956**, p 375.
[36].   Bohm, D. *op cit*, p 486.
[37].   *loc cit*, reference 41,

M$_3$(CO)$_4$ Bond Energies for First Row Transition Metal Series Elements.

Transition Metal String	Bond Energy (eV)	Bond Energy (eV)
Ti-Ti-Ti	+0.898	+1.105
V-V-V	-0.177	-0.185
Cr-Cr-Cr	+0.292	-0.595
Mn-Mn-Mn	-2.558	+2.812
Fe-Fe-Fe	-0.161	-2.504
Co-Co-Co	-0.141	+2.789
Ni-Ni-Ni	+3.718	+0.862
Cu-Cu-Cu	-0.896	-0.226
Co-Fe-Co	-0.061*	+2.674

* The Fe-CO bond distance was 1.90 Angstroms.

37. Cotton, F. A. *Chemical Applications of Group Theory*, Interscience Publishers: New York, **1964**, p 89ff.
38. Blyholder, G.; Lawless, M. *Langmuir* **1991** *7 (1)* 140-1.
39. Castro, M. *Int. J. Quantum Chem.* **1997** *64 (2)* 223.
40. It is interesting to note the use of the symbol σ$_d$ instead of the symbol σ$_v$ reflecting a somewhat arbitrary use of the notation in this regard.
41. Carter, M. K. *J. Molecular Catalysis A: Chemical* **2001** *172*, 193.
42. Boor, J. *Polymer Sci., Part D, 2* **1967** 115.
43. Landau, L. D.; Lifshitz, E. M. *Quantum Mechanics* , John Pergamon Press, Ltd.: London, **1958**, p. 306.
44. Cai, Xiaochen; Majumdar, Subhojit; Fortman, George C.; Cazin, Catherine S.J.; Slawin, Alexandra M.Z.; Lhermitte, Charles; Prabhakar, Rajeev; Germain, Meaghan E.; Palluccio, Taryn; Nolan, Steven P.; Rybak-Akivoma, Elena V.; Temprado, Manuel; Captain, Burjor; Hoff, Carl D. *J. Am. Chem.Soc.* **2011**, *133* (5), 1290; DOI: 10.1021/ja1103348.
45. Carter, M. K. *J. Molecular Catalysis A: Chemical* **2003** *200*, 191.
46. Pauling, L.; Wilson, E. B., loc cit, p 138.
47. Pauling, L. *J.Am.Chem.Soc.* **1932** *54*, 3570.
48. Pauling, L.; Wilson, E. B. *Introduction to Quantum Mechanics*, McGraw-Hill Book Co., New York, **1935**, pp 165-175.
49. Wei, C. H.; Dahl, L. F. *J. Am. Chem. Soc.* **1969** *91*, 1351.
50. Hehre, W. J.; Radom, L.; Schleyer, P. v. R.; Pople, J. A. *Ab Initio Molecular Orbital Theory*, John Wiley & Sons: New York, **1986**, p219.
51. Cotton, F. A. and Troup, J. M. *J. Am. Chem. Soc.* **1974** *96*, 3438.
52. Ball, J. I.; Morgan, C. H. *Acta Cryst.* **1967** *23*, 239.
53. Hehre, W. J.; Radom, L.; Schleyer, P. v. R.; Pople, J. A. *op cit*, p21.
54. Slater, J. C. *Quantum Theory of Atomic Structure*, Volume I; McGraw-Hill Book Company, Inc.: New York, **1960**, p25. Includes a detailed presentation on units.
55. Hehre, W. J.; Radom, L.; Schleyer, P. v. R.; Pople, J. A. *op cit*, p23.
56. Lewis, K. E. Golden, D. M.; Smith, K. P. *J. Am. Chem. Soc.* **1984** *106*, 3905.
57. Ehlers, A. W.; Frenking, G. *Organometallics* **1995** *14 (1)*, 423.
58. Schreckenbach, J.; Li, G.; Ziegler, T. *J. Am. Chem. Soc.* **1995** *117*, 486.
59. Sagi, I.; Chance, M. R. *J. Am. Chem. Soc* **1992** *114*, 8061.
60. Lee, S. C.; Holm, R. H. *Inorganic Chemistry* **1993** *32*, 4745.
61. Kitajima, N.; Fujisawa, K.; Fujimoto, C.; Moro-oka, Y.; Hashimoto, S.; Kitagawa, T.; Toriumi, K.; Tatsumi, K.; Nakamura, A. *J. Am. Chem. Soc.* **1992** *114*, 1277.
62. Benson, S. W. *The Foundations of Chemical Kinetics*, McGraw-Hill Book Company: New York, **1960**, p 218.
63. Benson, S. W. *op cit*, p 24.
64. Bohm, D. *Quantum Theory*, Prentice-Hall, Inc., Englewood Cliffs, NJ, **1956**, pp 27, 38, 412.
65. Eyring, H.; Walter, J.; Kimball, G. E. *Quantum Chemistry*, John Wiley & Sons, Inc., New York, **1963**, p 112.
66. Pauling, L.; Wilson, E. B. *Introduction to Quantum Mechanics*, McGraw-Hill Book Co., New York, **1935**, p 302.
67. Merzbacher, E. *Quantum Mechanics*, John Wiley & Sons: New York, **1961**, p 470.
68. Merzbacher, E. *op cit*, pp 452-481.

69. Greenwood, N. N.; Earnshaw, A. *Chemistry of the Elements*, Pergamon Press: New York, **1984**, Ch.2, p30.
70. Mulliken, R. S. *J.Chem.Phys.* **1934** *2*, 782; ibid **1935** 3, 573.
71. Moffitt, W. E. *Proc. Roy. Soc. A* **1949** *196*, 510.
72. Cotton, F. A.; Wilkinson, G. *Advanced Inorganic Chemistry*, John Wiley & Sons: New York, **1980**, 4th ed., pp 63, 1050.
73. *loc cit*, reference 45,

Relative Bonding Energies for First Row Transition Metal Complexes

Transition Metal Complex [*]	ΔE (eV)	ΔE (kcal/mol)
$Ti_2(O_2)_4^{4+}$	+0.0003	< +0.1
$V_2(O_2)_4^{4+}$	+0.6128	+14.1
$Cr_2(O_2)_4^{4+}$	+0.5327	+12.3
$Mn_2(O_2)_4^{4+}$	-0.1193	-2.7
$Fe_2(O_2)_4^{4+}$	+0.0482	+1.1
$FeCl_4^{2-}(O_2)_4FeCl_4^{2-}$ [**]	-6.476	-149.
$Co_2(O_2)_4^{4+}$	-0.2455	-5.7
$Ni_2(O_2)_4^{4+}$	-0.2312	-5.3
$Cu_2(O_2)_4^{4+}$	-0.9114	-21.0

[*] The optimized distances were d(M-M) = 0.2482 nm, d(O-O) = 0.125 nm.

[**] Bond distance for Fe-Cl is 0.265 nm and Cl-Fe-Cl bond angle is 102 degrees.

74. Carter, M. K. IOSR *J. Appl. Chem.* **2020** *13*, 11-27.
75. Carter, M. K. IOSR *J. Appl. Chem.* **2020** *13*, 1-10.

Appendix I. Figure 6 - Propene Dimerization on a Catalyst

Monomers

Intermediate

Dimer
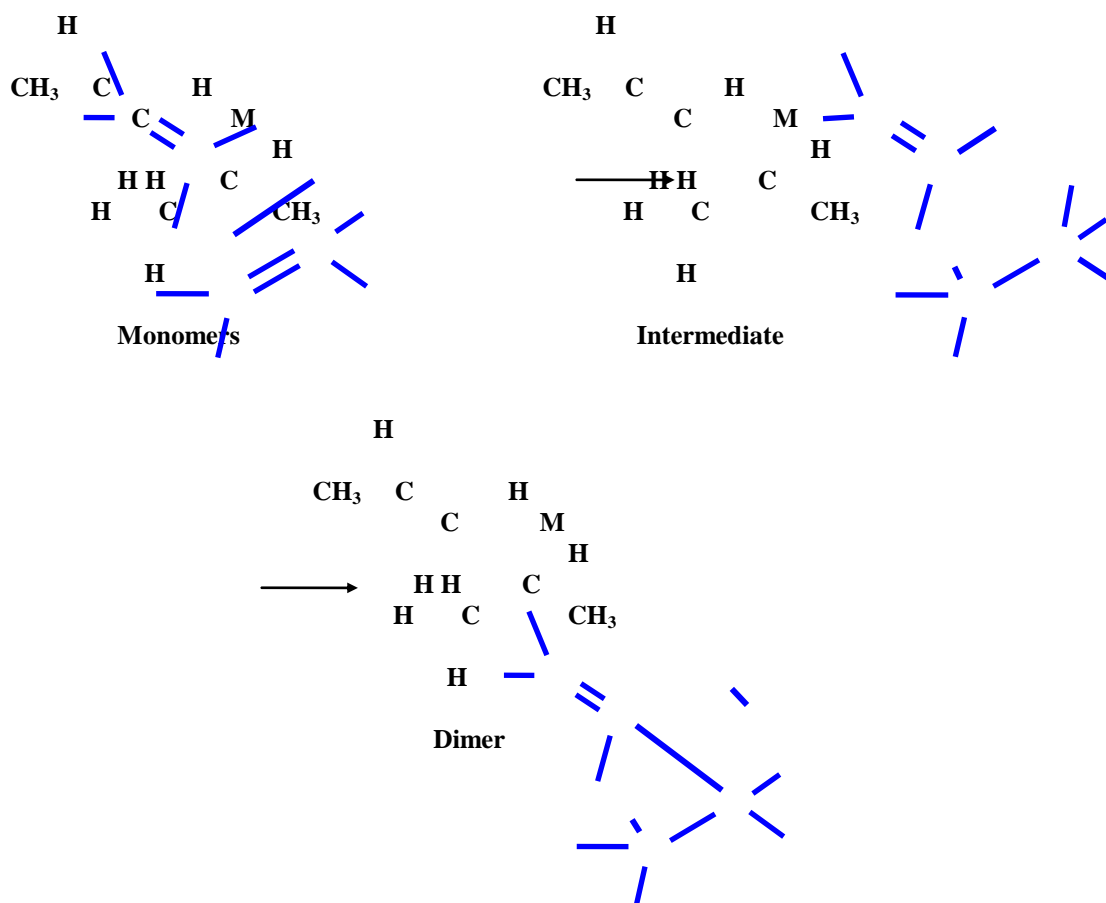
Table 2. C_{4v} Symmetry Group Character Table

	E	$2C_4$ (z)	C_2	$2\sigma_v$	$2\sigma_d$	linear, rotations	quadratic
A_1	1	1	1	1	1	z	x^2+y^2, z^2
A_2	1	1	1	-1	-1	R_z	
B_1	1	-1	1	1	-1		x^2-y^2
B_2	1	-1	1	-1	1		xy
E	2	0	-2	0	0	(x, y) (R_x, R_y)	(xz, yz)

$\Gamma_{CO} = A_1 + B_1 + E$ and $\Gamma_{Fe} = 2A_1$

Table 3. D_{4h} Symmetry Group Character Table

	E	$2C_4$ (z)	C_2	$2C'_2$	$2C''_2$	i	$2S_4$	σ_h	$2\sigma_v$	$2\sigma_d$	linears, rotations	quadratic
A_{1g}	1	1	1	1	1	1	1	1	1	1		x^2+y^2, z^2
A_{2g}	1	1	1	-1	-1	1	1	1	-1	-1	R_z	
B_{1g}	1	-1	1	1	-1	1	-1	1	1	-1		x^2-y^2
B_{2g}	1	-1	1	-1	1	1	-1	1	-1	1		xy
E_g	2	0	-2	0	0	2	0	-2	0	0	(R_x, R_y)	(xz, yz)
A_{1u}	1	1	1	1	1	-1	-1	-1	-1	-1		
A_{2u}	1	1	1	-1	-1	-1	-1	-1	1	1	z	
B_{1u}	1	-1	1	1	-1	-1	1	-1	-1	1		
B_{2u}	1	-1	1	-1	1	-1	1	-1	1	-1		
E_u	2	0	-2	0	0	-2	0	2	0	0	(x, y)	